The Astrophysical Journal Letters, 887:L32 (5pp), 2019 December 20 https://doi.org/10.3847/2041-8213/ab59dd

Variable Warm Dust around the Herbig Ae Star HD 169142: Birth of a Ring?*

Lei Chen[1], Attila Moór[1], Alexander Kreplin[2], Ágnes Kóspál[1,3], Peter Ábrahám[1], Alexis Matter[4], Andres Carmona[5,6], Karl-Heinz Hofmann[7], Dieter Schertl[7], and Gerd Weigelt[7]

[1] Konkoly Observatory, Research Centre for Astronomy and Earth Sciences, Konkoly-Thege Miklós út 15-17, 1121 Budapest, Hungary; lei.chen@csfk.mta.hu
[2] University of Exeter, Department of Physics and Astronomy, Stocker Road, Exeter, Devon EX4 4QL, UK
[3] Max Planck Institute for Astronomy, Königstuhl 17, D-69117 Heidelberg, Germany
[4] Laboratoire Lagrange, UMR7293, Université de Nice Sophia-Antipolis, CNRS, Observatoire de la Côte d'Azur, F-06300 Nice, France
[5] Institut de Planétologie et d'Astrophysique de Grenoble, Université Grenoble Alpes, CS 40700, F-38058 Grenoble Cédex 9, France
[6] L'Institut de Recherche en Astrophysique et Planétologie, 9, avenue du Colonel Roche, BP 44346-31028 Toulouse Cedex 4, France
[7] Max-Planck-Institut für Radioastronomie, Auf dem Hügel 69, D-53121 Bonn, Germany
Received 2019 November 3; revised 2019 November 18; accepted 2019 November 21; published 2019 December 17

Abstract

The Herbig Ae star HD 169142 is known to have a gaseous disk with a large inner hole, and also a photometrically variable inner dust component in the sub-astronomical-unit region. Following up on our previous analysis, we further studied the temporal evolution of inner dust around HD 169142, which may provide information on the evolution from late-stage protoplanetary disks to debris disks. We used near-infrared interferometric observations obtained with the Very Large Telescope Interferometer/PIONIER to constrain the dust distribution at three epochs spanning six years. We also studied the photometric variability of HD 169142 using our optical–infrared observations and archival data. Our results indicate that a dust ring at ∼0.3 au formed some time between 2013 and 2018, and then faded (but did not completely disappear) by 2019. The short-term variability resembles that observed in extreme debris disks, and is likely related to short-lived dust of secondary origin, though variable shadowing from the inner ring could be an alternative interpretation. If confirmed, this is the first direct detection of secondary dust production inside a protoplanetary disk.

Unified Astronomy Thesaurus concepts: Pre-main sequence stars (1290); Herbig Ae/Be stars (723); Protoplanetary disks (1300); Debris disks (363)

1. Introduction

During their lifetimes of several million years, protoplanetary disks gradually lose their primordial gas and dust components, often developing gap or hole structures (Alexander et al. 2014). Finally they evolve into debris disks, whose emission is dominated by second-generation dust released by collisional cascades following the collision of large parental bodies, i.e., planetesimals (Krivov 2010; Hughes et al. 2018). Wyatt et al. (2015) pointed out that the creation of second-generation dust might start in the protoplanetary phase, and could be a possible origin of inner hot dust in pretransitional disks. In this paper we report evidence of second-generation dust production in the Herbig Ae star HD 169142.

HD 169142 (see stellar parameters in Table 1) is an intermediate-mass young star with peculiar disk structure, which has been intensively studied in recent years. In radio and in scattered light, the dusty disk has a morphology with a large inner hole of ∼20 au and multiple gaps (Honda et al. 2012; Quanz et al. 2013; Momose et al. 2015; Fedele et al. 2017; Monnier et al. 2017; Pérez et al. 2019). Planet candidates have been found in the gap regions (Biller et al. 2014; Osorio et al. 2014; Reggiani et al. 2014). Recent VLT/SPHERE observations revealed an even more complex circumstellar structure with blobs, rings, and spiral arms (Ligi et al. 2018; Gratton et al. 2019). The hole and gaps, together with the advanced age (6^{+6}_{-3} Myr, Grady et al. 2007), suggest that the disk has evolved to a late-stage protoplanetary disk. Recently, A. Carmona et al. (2019, in preparation) found the inner ∼20 au to be gas-depleted, with a gas surface density of only 10^{-5}–10^{-3} g cm^{-2}, three to five orders of magnitude lower than that at $R \gtrsim 20$ au.

Despite its evolved state and the significant gas clearing of the inner ∼20 au region, HD 169142 still has a near-infrared (NIR) excess, indicating the existence of warm dust ($T \sim 1500$ K) in the sub-astronomical-unit inner disk region. Wagner et al. (2015) revealed a fading trend in the NIR, indicating that the inner warm dust has lost half of its fractional luminosity in no more than 10 yr. With NIR interferometry, we constrained the location and grain size distribution of the dust (Chen et al. 2018), finding it most likely to be optically thin dust located at ∼0.08 au from the central star, consisting of mainly large dust grains (>1 μm). We further speculated that the dust might consist of second-generation grains released by collisional cascades following collisional events between planetesimals.

In 2018 and 2019 we performed new observations of HD 169142, including NIR interferometric observations with the Very Large Telescope Interferometer (VLTI)/PIONIER and photometric observations with the Small and Moderate Aperture Research Telescope System (SMARTS) 1.3 m telescope. Complementing these with archival data, we found new evidence for variations in the amount and spatial distribution of the warm dust, indicating that the dust is experiencing much more frequent and short-term changes than previously found. In the present paper, we report on the modeling and interpretation of the new data set.

2. Observations and Results

2.1. VLTI/PIONIER Interferometric Observations

We observed HD 169142 with the ESO VLTI and its *H*-band four-beam combiner PIONIER (Le Bouquin et al. 2011), under

* Based on observations collected at the European Organisation for Astronomical Research in the Southern Hemisphere under ESO programs 0101.C-0367 and 60.A-9135.

Table 1
Stellar Parameters of HD 169142

Parameter	Value	Reference
distance	113.6 ± 0.8 pc	a
Sp. Type	A5V	b
M_*	1.65 $M_\odot$	c
L_*	5.2 $L_\odot$	d
$T_{\rm eff}$	7500 K	c
Age	6^{+6}_{-3} Myr	e
Disk Inclination	13°	f

References. (a) Bailer-Jones et al. (2018); (b) Dunkin et al. (1997); (c) Wagner et al. (2015); (d) Chen et al. (2018); (e) Grady et al. (2007); (f) Raman et al. (2006).

ESO program 0101.C-0367 (PI: L. Chen; performed on 2018 August 10) and 60.A-9135 (PI: L. Chen; performed between 2019 April 27 and 2019 May 12). The program 60.A-9135 was a science verification project of the NAOMI adaptive optics systems (Woillez et al. 2019). The data was reduced and calibrated with the PNDRS package (Le Bouquin et al. 2011).

In Figure 1 we show the measured interferometric visibilities, which are lower than the previous measurements on similar baselines in 2011 and 2013 (Lazareff et al. 2017). The changes of visibility with time indicate changes in the amount/distribution of inner dust, which will be further modeled in Section 4 and discussed in later sections.

2.2. Optical–Infrared Photometric Observations

We observed HD 169142 on the night of 2019 June 23 using the 1.3 meter telescope of the SMARTS at Cerro Tololo, Chile, in the $IJHK_s$ bands. We obtained aperture photometry in the images and converted the instrumental magnitudes to standard ones using several comparison stars in the field of view. In the I band, we converted the *Gaia* G, RP, and BP magnitudes of the comparison stars to Johnson–Cousins I magnitudes using transformation equations from the *Gaia* web page,[8] while in the JHK_s bands, we used the 2MASS magnitudes of the comparison stars. The resulting magnitudes are $I = 7.72 \pm 0.02$, $J = 7.45 \pm 0.02$, $H = 7.10 \pm 0.02$, and $K_s = 6.77 \pm 0.03$. Compared with its spectral energy distribution in 2013 (Lazareff et al. 2017), HD 169142 brightened in the K_s band by ∼0.1 mag, while exhibiting no significant variability in the IJH bands.

2.3. WISE Archival Infrared Data

We searched for photometric observations of HD 169142 in the archive of the *Wide-field Infrared Survey Explorer* (*WISE*; Wright et al. 2010), through the AllWISE Multiepoch Photometry table and *NEOWISE*-R Single Exposure (L1b) Source table,[9] and plotted light curves of HD 169142 in the *WISE W1* (3.4 μm) and *W2* (4.6 μm) bands (Figure 2).

The light curves show strong variability, including a rapid brightening in 2010, and a slow brightening from 2014 to 2018. However, *WISE* photometry measurements of HD 169142 have to be considered with caution. The object is very bright, leading to detector saturation. Moreover, the lack of cooling during the *NEOWISE* Reactivation mission further degraded the data quality. In this brightness range there is a known systematic offset between the *NEOWISE* Reactivation and AllWISE photometry (Mainzer et al. 2014). In order to examine the reliability of the observed changes in *NEOWISE* Reactivation we selected a sample of comparison stars with the following criteria: (1) within a distance of <6° to HD 169142;

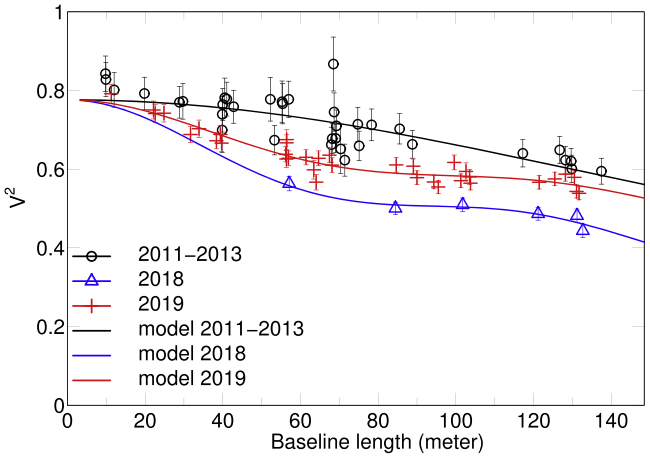

Figure 1. *H*-band visibilities from the VLTI/PIONIER observations of HD 169142 in 2018 and 2019, and our star–ring–ring–halo model fitting. Earlier VLTI observations from 2011 to 2013 and our previous model (Chen et al. 2018) are plotted for comparison.

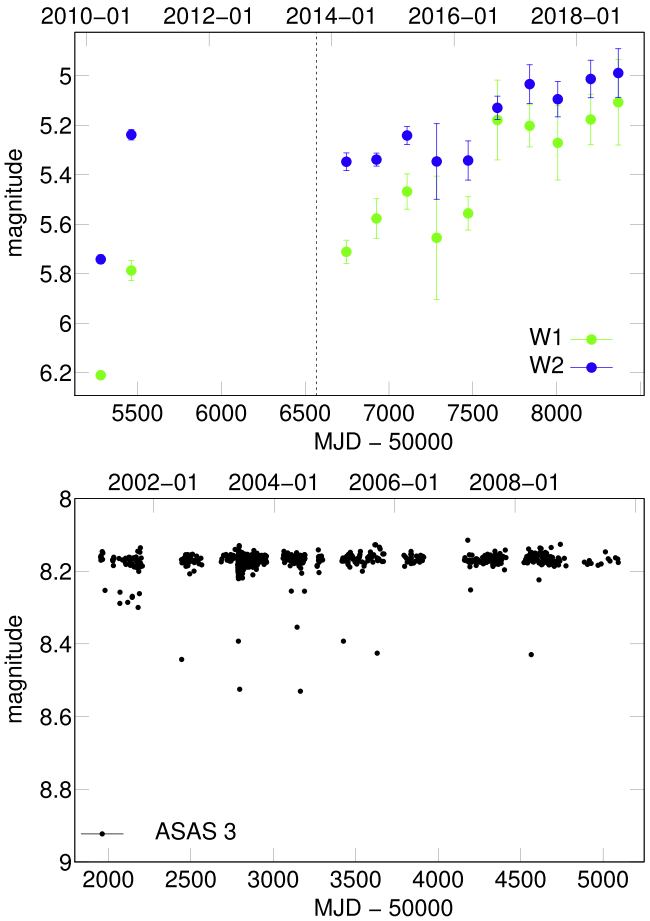

Figure 2. Light curves of HD 169142. Upper panel: *WISE* and *NEOWISE* observations. The vertical dashed line indicates the start of the *NEOWISE* Reactivation mission. The data points within each mission phase are binned to reduce the noise. Lower panel: ASAS-3 observations.

[8] https://gea.esac.esa.int/archive/documentation/GDR2/Data_processing/chap_cu5pho/sec_cu5pho_calibr/ssec_cu5pho_PhotTransf.html

[9] Both accessible from the IRSA web page https://irsa.ipac.caltech.edu/.

(2) spectral type between B8 and F3; (3) and AllWISE *W1*-band magnitudes between 5.45 and 6.95 mag (6.2 ± 0.75 mag). AllWISE sources flagged as seriously contaminated (judged from the field "cc_flag") in the *W1* or *W2* band were discarded from the sample. This left us with 29 comparison stars. Using the IRSA database we then gathered all single exposure photometric data for the selected stars and derived one photometric data point for each mission phase by averaging the single exposure photometric data (using only the good quality measurements). We computed the Stetson index (Stetson 1996; Sokolovsky et al. 2017) for each object using the obtained *W1* and *W2* band data pairs in the *NEOWISE* Reactivation. For nonvariable objects with random noise, no correlation is expected between the different band observations. Therefore, their Stetson index should be close to zero. In case of real correlated variability, the index should be positive. The Stetson index we found for HD 169142 is 0.64, while those for the comparison stars range from −0.13 to 0.29. The high Stetson index of our target suggests that its observed changes are significant.

2.4. Gaia *Archival Data*

We retrieved optical photometric information of HD 169142 from *Gaia* DR2 (Gaia Collaboration et al. 2016, 2018). The mean G magnitude in DR2 is 8.054, with flux accuracy of $(f/\delta f)_{\rm G} = 1081$. These are combined photometric information from the 129 good observations during the DR2 period (2014 July 25 to 2016 May 23), while the individual results are not public. Following the method of Deason et al. (2017), we estimated the flux scatter of multiepoch *Gaia* observations as $\Delta f/f = \sqrt{N_{\rm obs}}\,\delta f/f = 1.0\%$. The low flux scatter indicates HD 169142 to be quite stable in G band during the ∼22 months of *Gaia* DR2 observations.

2.5. ASAS Optical Monitoring

We collected V- and g-band photometric observations of HD 169142 from the ASAS-3 (Pojmanski 1997) and ASAS-SN (Shappee et al. 2014; Kochanek et al. 2017) databases. In the ASAS-3 observations (Figure 2), HD 169142 appears to be stable at most epochs at $V = 8.17 \pm 0.02$ mag, but encounters sporadic fading events. However, similar sporadic fading is ubiquitously seen in ASAS light curves of stars with similar brightness in the nearby region. Therefore, instead of true fading, these are more likely due to artifacts. ASAS-SN measurements for HD 169142 are saturated; therefore, we did not use them. Overall, we do not see any reliable evidence of optical variability.

3. Infrared Photometric Variability

The data set we collected suggests that HD 169142 is stable in the optical, but likely has complex variability in the NIR. While Wagner et al. (2015) have already revealed an NIR fading of HD 161942 from pre-2000 to post-2000, we found that the object might have exhibited further flux changes in the NIR since 2010. In the *WISE* light curves (Figure 2), the object seems to be brightening in 2010, and also brightened between 2014 and 2018. The object also brightened slightly in K_s band from 2013 to 2019, but did not exhibit a clear variability in J and H bands. In summary, the NIR variability of HD 169142 likely consists of a series of fluctuations, rather than a monotonic fading, and the variability does not appear to be monochromatic. Specifically, a component that emits mainly at K band and longer wavelengths might have arisen in the past 5 years.

4. Modeling of the Interferometric Data

In this section we present our modeling of the H-band interferometric visibilities from 2018 and 2019, which constrains the location of warm dust and its flux ratio to the central star. The differences in the data sets indicate that significant structural changes happened not only between 2013 and 2018, but also between 2018 and 2019. Therefore, the 2018 and 2019 data sets have to be modeled separately. The small data set in 2018 leaves large ambiguity in modeling, while the 2019 data set can constrain the radial distribution much better.

4.1. Modeling the 2019 Data Set

The 2019 data set indicates a radial brightness distribution quite different from that in 2011–2013. A prominent difference is the steeper drop of visibility with increasing baseline length from zero to ∼60 m, suggesting a component that is larger than the ring structure at 0.065 mas in our previous model (Chen et al. 2018) and is resolved at ∼60 m. In order to account for this additional component, in the following we used a model that consists of the star, an inner ring, an outer ring, and a halo component. For each ring, we assumed a uniform brightness between its inner radius $r_{\rm in}$ and outer radius $r_{\rm out}$. We used the mean radius $r_{\rm ring} = (r_{\rm in} + r_{\rm out})/2$ as the model parameter, and assumed $r_{\rm in} = 0.9 r_{\rm ring}$ and $r_{\rm out} = 1.1 r_{\rm ring}$ to implement a ∼20% width.

We denoted the flux from the four components as $F_{\rm star}$, $F_{{\rm ring},i}$, and $F_{\rm halo}$, where i is either 1 (inner ring) or 2 (outer ring). We defined

$$k_{{\rm ring},i} = \frac{F_{{\rm ring},i}}{F_{\rm star}},\ i = 1, 2, \tag{1}$$

and

$$k_{\rm halo} = \frac{F_{\rm halo}}{F_{\rm star} + \sum_i F_{{\rm ring},i}}. \tag{2}$$

Therefore, the total flux is

$$\begin{aligned} F_{\rm total} &= F_{\rm star} + \sum_i F_{{\rm ring},i} + F_{\rm halo} \\ &= (1 + \sum_i k_{{\rm ring},i})(1 + k_{\rm halo}) F_{\rm star}. \end{aligned} \tag{3}$$

The visibility on a given baseline length B is

$$\begin{aligned} V &= \frac{F_{\rm star} V_{\rm star} + \sum_i F_{{\rm ring},i} V_{{\rm ring},i} + F_{\rm halo} V_{\rm halo}}{F_{\rm total}} \\ &= \frac{V_{\rm star} + \sum_i k_{{\rm ring},i} V_{{\rm ring},i} + k_{\rm halo}(1 + \sum_i k_{{\rm ring},i}) V_{\rm halo}}{\left(1 + \sum_i k_{{\rm ring},i}\right)(1 + k_{\rm halo})}. \end{aligned} \tag{4}$$

As an approximation we took $V_{\rm star} \equiv 1$ and $V_{\rm halo} \equiv 0$. For the visibility of each ring we used the Bessel function

$$V_{\rm ring} = 2\frac{x_{\rm out} J_1(x_{\rm out}) - x_{\rm in} J_1(x_{\rm in})}{x_{\rm out}^2 - x_{\rm in}^2}, \tag{5}$$

where $x_{\rm in} = 2\pi\nu r_{\rm in}$, $x_{\rm out} = 2\pi\nu r_{\rm out}$, and $\nu = B/\lambda$ is the spatial frequency; B is the baseline length, and λ is the wavelength.

Table 2
Results of Our Modeling of the Visibilities of HD 169142 from 2018 and 2019 with the Star–Ring–Ring–Halo Model

Parameter	2011–2013	2018	2019
$k_{\rm halo}$ (%)	13.5	13.5	13.5
$k_{\rm ring,1}$ (%)	28.7	43.5 ± 5.3	24.8 ± 2.8
$k_{\rm ring,2}$ (%)	0	15.0 ± 1.3	8.2 ± 0.5
$r_{\rm ring,1}$ (mas)	0.655	0.655	0.655
$r_{\rm ring,2}$ (mas)	0	2.86 ± 0.21	2.73 ± 0.14
$f_{\rm star}$ (%)	68.5	55.6 ± 1.7	66.2 ± 1.2
$f_{\rm halo}$ (%)	11.9	11.9	11.9
$f_{\rm ring,1}$ (%)	19.6	24.2 ± 2.3	16.4 ± 1.6
$f_{\rm ring,2}$ (%)	0	8.3 ± 0.9	5.4 ± 0.4
$R_{\rm ring,1}$ (au$\left(\frac{d}{113.6\ {\rm pc}}\right)$)	0.074	0.074	0.074
$R_{\rm ring,2}$ (au$\left(\frac{d}{113.6\ {\rm pc}}\right)$)	0	0.32 ± 0.02	0.31 ± 0.02
χ^2	···	2.53	36.9
$\chi^2_{\rm red}$	···	0.84	1.12

Note. The uncertainties of the parameters are estimated with the bootstrapping method. The best-fit model parameters for the 2011–2013 observations (Chen et al. 2018) are listed for comparison.

Overall, the model visibilities are determined by five model parameters $k_{\rm halo}$, $k_{{\rm ring},i}$, and $r_{{\rm ring},i}$.

We fitted the 2019 data set by adjusting $k_{\rm ring,1}$, $k_{\rm ring,2}$, and $r_{\rm ring,2}$, while keeping $k_{\rm halo}$ and $r_{\rm ring,1}$ fixed to the values in model 2011–2013. The reasons to fix $k_{\rm halo}$ are as follows. First, this parameter mainly accounts for the scattered light from the outer disk at $\gtrsim$20 au, which has a dynamical timescale of ∼100 yr and is therefore not expected to change during the observations. Second, in the 2019 observations, the visibility does appear to converge while $B \to 0$ to roughly the same level as that for 2011–2013. We fixed the location of the inner ring at the value from the 2011–2013 model, which is roughly the dust sublimation radius. This ring is barely resolved by our observations, leading to a degeneracy between its size and its flux ratio in the modeling. The parameters of our best-fit model are presented in Table 2. Besides the model parameters, we also list several derived quantities, including the flux ratio of each model component, and the linear size of each ring. The modeled visibility curve is plotted in Figure 1 (red curve). The model reproduces the observations within the formal uncertainties, accounting for the steep drop of visibility at the short baselines with the outer ring at ∼0.3 au. For comparison, our previous model of the 2011–2013 VLTI/PIONIER observations (model 2011–2013; Chen et al. 2018) is also listed.

4.2. Modeling the 2018 Data Set

Considering the hints from the 2019 modeling, we modeled the 2018 data set with a similar two-ring model, and again assumed $k_{\rm halo}$ and $r_{\rm ring,1}$ to be the same as in model 2011–2013. The model parameters are shown in Table 2 and the resulting model visibilities are plotted in Figure 1 (blue curve). Again, an outer ring at $\gtrsim$0.3 au is clearly required for fitting the data; however, the flux of the outer ring is higher by a factor of ∼2 than that in model 2019.

Due to the lack of measurements with short baselines, the size of the outer ring cannot be unambiguously constrained.

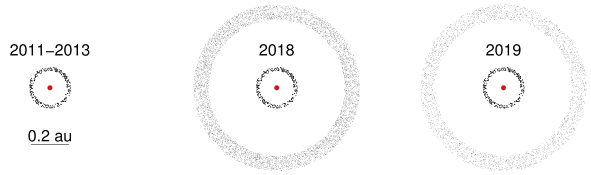

Figure 3. Sketch for the temporal changes in dust distribution. An outer dust ring at ∼0.3 au formed some time between 2013 and 2018, and then faded by 2019.

The data can also be roughly reproduced with much larger $r_{\rm ring,2}$. The $r_{\rm ring,2}$ value in Table 2 was obtained with the artificial constraint that it must not exceed 4 mas, and therefore should be understood as a lower limit. However, when radiative equilibrium is considered, it is likely that the ring radius cannot be much larger than ∼0.3 au, because a large distance to the star will make the dust too cold to emit in the NIR.

5. Discussion

5.1. A Scenario of Dust Evolution

Combining the interferometric and photometric observations described above, the inner dust in HD 169142 likely experienced a variation as shown in Figure 3. The inner dust ring at ∼0.08 au stays almost constant over time. An outer dust ring at ∼0.3 au formed some time between 2013 and 2018, and then faded (but did not completely disappear) by 2019. Due to the larger distance to the central star, the outer ring is colder ($T \lesssim 1000$ K) than the inner one ($T \sim 1500$ K). Therefore, it emits mainly at wavelengths longer than ∼2 μm, explaining the brightening in *K* band and *WISE W1/W2* bands, while not causing variability in *IJ* bands. In the *H* band, in order to reproduce the interferometric data, a flux contribution from the outer ring of 15% in 2018 and 8% in 2019 is required, which should have caused a brightening in 2018 relative to 2013. The lack of *H*-band variability between the 2013 SAAO and 2019 SMARTS observations could be due to a simultaneous slight fading of the innermost ring, but could also be related to observational uncertainty.

5.2. Resemblance to Extreme Debris Disks

We compared the observational characteristics of the inner dust of HD 169142 with those of the extreme debris disks (EDDs) and found a similarity. EDDs are a new class of debris disks with high fractional luminosities of $f_{\rm IR} \gtrsim 10^{-2}$, discovered in recent years (see, e.g., Hughes et al. 2018, and reference therein). Short-term variability is frequently found in these objects. One spectacular case is TYC8241 2652 1, whose IR excess has been as strong as $f_{\rm IR} \approx 11\%$ but then dropped by at least a factor of 30 to an undetectable level within two years (Melis et al. 2012). Another extreme debris disk, 2MASS J08090250−4858172 (also known as [GBR2007] ID8) brightened in 2012 and then gradually faded in 2013 (Meng et al. 2012, 2014). In a sample study of extreme debris disks (Meng et al. 2015), four out of the five targets exhibit variability over the ∼1 yr period of observation. Therefore, variability on yearly timescales is common, if not ubiquitous, among EDDs.

The sub-astronomical-unit warm dust of HD 169142 is variable on timescale of 1–10 yr, and has a fractional luminosity of several to 10%. It is located at one to several 0.1 au, and has a temperature of ∼1500 K or slightly less.

These characteristics are similar to those of the EDDs, suggesting this dust consists of short-lived second-generation grains released by planetesimal collision events.

While HD 169142 has a massive gaseous outer disk, its inner ~20 au is gas-depleted (see Section 1). In particular, A. Carmona et al. (2019, in preparation) found the gas surface density in the innermost <1 au region to be only $\sim 10^{-5}$ g cm^{-2} (though with an upper limit of $\sim 10^{-3}$ g cm^{-2}). This low surface density is consistent with our scenario that the sub-astronomical-unit dust of HD 169142 is secondary dust formed in a gas-poor environment, rather than primordial dust coupled with gas.

Besides true changes in dust amount in the ~0.3 au ring, another possible mechanism for the photometric variability would be a temporally variable shadowing from the inner ring, which might be related to precessing of misaligned disk components. Theoretical studies suggest that an inclined massive planet could break up the disk into misaligned components and cause differential precession of the components (e.g., Zhu 2019). Garufi et al. (2019) found a wiggling in the jet of the T Tauri star RY Tau, and proposed that a giant planet at sub-astronomical-unit scales could cause a precession of the inner disk with timescale of ~30 yr, and be responsible for the jet wiggling. In the case of HD 169142, the inner ~0.08 au ring would cast a variable shadow on the ~0.3 au outer ring if both components are precessing differentially. Future photometric monitoring will help to verify the two competing scenarios, because the precession scenario suggests a well-defined period, while the collisional event scenario suggests episodical brightening and fading.

5.3. An Ideal Laboratory of Short-term Dust Evolution

As mentioned above, HD 169142 might be experiencing short-term dust evolution similar to those in EDDs. While the physical processes might be similar, there is a large difference in observability between HD 169142 and the known EDDs. As an A type star at a distance of ~100 pc, HD 169142 is much brighter than most known EDDs, and its inner dust has much larger angular size. Therefore, its inner dust can be readily spatially resolved with VLTI, which provides a unique opportunity for detailed studies of a rapidly evolving warm circumstellar dust, employing multiepoch, spatially resolved observations.

6. Summary

We used NIR interferometric observations with VLTI/PIONIER to constrain the dust distributions in the inner sub-astronomical-unit region of HD 169142 in 2018 and 2019 and compared them with that in 2011–2013. In both the 2018 and 2019 observations, evidence was found for a dust ring at ~0.3 au, which was not seen in 2011–2013. Photometric data indicates a brightening at wavelengths longer than >2 μm, but no significant variability at shorter wavelengths. Therefore, the whole data set favors a scenario that a dust ring at ~0.3 au formed at some time between 2013 and 2018, and then faded (but did not completely disappear) by 2019. The short-term variability resembles those observed in extreme debris disks. This finding makes HD 169142 a unique laboratory for studying the short-term physical processes affecting the nature of dust during the late stages of the protoplanetary phase.

This project has received funding from the European Research Council (ERC) under the European Union's Horizon 2020 research and innovation programme under grant agreement No. 716155 (SACCRED). A.K. acknowledges support from ERC Starting Grant (grant agreement No. 639889). Our work was supported by the Hungarian OTKA grant K132406. This work has made use of data from the European Space Agency (ESA) mission *Gaia* (https://www.cosmos.esa.int/gaia), processed by the *Gaia* Data Processing and Analysis Consortium (DPAC; https://www.cosmos.esa.int/web/gaia/dpac/consortium). Funding for the DPAC has been provided by national institutions, in particular the institutions participating in the *Gaia* Multilateral Agreement. We are grateful to an anonymous referee for useful comments.

Facilities: VLTI(PIONIER), SMARTS, *WISE*, *Gaia*, ASAS.

ORCID iDs

Lei Chen https://orcid.org/0000-0003-2835-1729
Alexander Kreplin https://orcid.org/0000-0002-0911-9505
Ágnes Kóspál https://orcid.org/0000-0001-7157-6275
Peter Ábrahám https://orcid.org/0000-0001-6015-646X
Gerd Weigelt https://orcid.org/0000-0001-9754-2233

References

Alexander, R., Pascucci, I., Andrews, S., Armitage, P., & Cieza, L. 2014, in Protostars and Planets VI, ed. H. Beuther, R. S. Klessen, C. P. Dullemond, & T. Henning, 475 (Tucson, AZ: Univ. Arizona Press)
Bailer-Jones, C. A. L., Rybizki, J., Fouesneau, M., Mantelet, G., & Andrae, R. 2018, AJ, 156, 58
Biller, B. A., Males, J., Rodigas, T., et al. 2014, ApJL, 792, L22
Chen, L., Kóspál, Á, Ábrahám, P., et al. 2018, A&A, 609, A45
Deason, A. J., Belokurov, V., Erkal, D., Koposov, S. E., & Mackey, D. 2017, MNRAS, 467, 2636
Dunkin, S. K., Barlow, M. J., & Ryan, S. G. 1997, MNRAS, 290, 165
Fedele, D., Carney, M., Hogerheijde, M. R., et al. 2017, A&A, 600, A72
Gaia Collaboration, Brown, A. G. A., Vallenari, A., et al. 2018, A&A, 616, A1
Gaia Collaboration, Prusti, T., de Bruijne, J. H. J., et al. 2016, A&A, 595, A1
Garufi, A., Podio, L., Bacciotti, F., et al. 2019, A&A, 628, A68
Grady, C. A., Schneider, G., Hamaguchi, K., et al. 2007, ApJ, 665, 1391
Gratton, R., Ligi, R., Sissa, E., et al. 2019, A&A, 623, A140
Honda, M., Maaskant, K., Okamoto, Y. K., et al. 2012, ApJ, 752, 143
Hughes, A. M., Duchêne, G., & Matthews, B. C. 2018, ARA&A, 56, 541
Kochanek, C. S., Shappee, B. J., Stanek, K. Z., et al. 2017, PASP, 129, 104502
Krivov, A. V. 2010, RAA, 10, 383
Lazareff, B., Berger, J. P., Kluska, J., et al. 2017, A&A, 599, A85
Le Bouquin, J. B., Berger, J. P., Lazareff, B., et al. 2011, A&A, 535, A67
Ligi, R., Vigan, A., Gratton, R., et al. 2018, MNRAS, 473, 1774
Mainzer, A., Bauer, J., Cutri, R. M., et al. 2014, ApJ, 792, 30
Melis, C., Zuckerman, B., Rhee, J. H., et al. 2012, Natur, 487, 74
Meng, H. Y. A., Rieke, G. H., Su, K. Y. L., et al. 2012, ApJL, 751, L17
Meng, H. Y. A., Su, K. Y. L., Rieke, G. H., et al. 2014, Sci, 345, 1032
Meng, H. Y. A., Su, K. Y. L., Rieke, G. H., et al. 2015, ApJ, 805, 77
Momose, M., Morita, A., Fukagawa, M., et al. 2015, PASJ, 67, 83
Monnier, J. D., Harries, T. J., Aarnio, A., et al. 2017, ApJ, 838, 20
Osorio, M., Anglada, G., Carrasco-González, C., et al. 2014, ApJL, 791, L36
Pérez, S., Casassus, S., Baruteau, C., et al. 2019, AJ, 158, 15
Pojmanski, G. 1997, AcA, 47, 467
Quanz, S. P., Avenhaus, H., Buenzli, E., et al. 2013, ApJL, 766, L2
Raman, A., Lisanti, M., Wilner, D. J., Qi, C., & Hogerheijde, M. 2006, AJ, 131, 2290
Reggiani, M., Quanz, S. P., Meyer, M. R., et al. 2014, ApJL, 792, L23
Shappee, B. J., Prieto, J. L., Grupe, D., et al. 2014, ApJ, 788, 48
Sokolovsky, K. V., Gavras, P., Karampelas, A., et al. 2017, MNRAS, 464, 274
Stetson, P. B. 1996, PASP, 108, 851
Wagner, K. R., Sitko, M. L., Grady, C. A., et al. 2015, ApJ, 798, 94
Woillez, J., Abad, J. A., Abuter, R., et al. 2019, A&A, 629, A41
Wright, E. L., Eisenhardt, P. R. M., Mainzer, A. K., et al. 2010, AJ, 140, 1868
Wyatt, M. C., Panić, O., Kennedy, G. M., & Matrà, L. 2015, Ap&SS, 357, 103
Zhu, Z. 2019, MNRAS, 483, 4221